SAND2022-11501C

HEAT TREATMENT EFFECTS ON MECHANICAL PROPERTIES OF WIRE ARC ADDITIVE MANUFACTURED Ti-6Al-4V

Natalia Saiz*, Jonathan Pegues*, Shaun Whetten*, Andrew Kustas*, Tyler Chilson†

*Material, Physical, and Chemical Sciences Center, Sandia National Laboratories, Albuquerque, NM 87185, USA

†ND Modernization & Future Systems, Sandia National Laboratories, Livermore, CA, USA

Abstract

Directed energy deposition (DED) is an attractive additive manufacturing (AM) process for large structural components. The rapid solidification and layer-by-layer process associated with DED results in non-ideal microstructures, such as large grains with strong crystallographic textures, resulting in severe anisotropy and low ductility. Despite these challenges, DED has been identified as a potential solution for the manufacturing of near net shape Ti-6Al-4V preforms. In this work, we explore several heat treatment processes, and their effects on tensile properties of wire arc additively manufactured (WAAM) Ti-6Al-4V. A high throughput tensile testing procedure was utilized to generate statistically relevant data sets related to each specific heat treatment and sample orientation. Results are discussed in the context of microstructural evolution and the resulting fracture behavior for each condition as compared to conventionally processed Ti-6Al-4V.

Introduction

Large format additive manufacturing (AM) using wire-based feedstock has become increasingly popular for the manufacture of titanium alloy preforms reducing both waste and lead time associated with conventional casting and forging processes. A common wire feed AM process is Wire Arc Additive Manufacturing (WAAM), which leverages typical welding energy sources such as MIG, TIG, plasma, or laser [1-4]. Wire directed energy deposition (W-DED) Ti-6Al-4V often form large columnar prior beta (β) grains that encourage continuous alpha (α) grain formation along the beta grain boundaries. The size of the continuous alpha grains is mostly influenced by the cooling rate from the beta phase field with the highest cooling rates resulting in the smallest continuous alpha in highly anisotropic mechanical properties.

The primary influence on strength for Ti-alloys is concentration of interstitial oxygen which can be of notable concern for welding AM processes that rely on shielding gasses to prevent significant oxidation during fabrication. The increase in oxygen and therefore strength is accompanied by severe reductions in ductility. Alpha lamella width, grain size, and colony size also play an important role in Ti-6Al-4V mechanical properties. The slip length, which is governed by the size of the grain/colony or lamella width, results in increasing strength and ductility with decreasing size. As such, high cooling rates from the beta field are favored over slower cooling rates. Conversely, extreme cooling rates result in martensitic transformation

resulting in acicular grains with high dislocation densities. These characteristics increase the strength of the alloy but have a deleterious impact on ductility and are therefore unfavorable for most applications.

For W-DED Ti-6Al-4V the large columnar prior beta grains and associated continuous alpha are the primary concern. These AM processes typically have more restrictions on deposition paths and lower cooling rates than powder-based AM processes, which is advantageous to continuous alpha formation and growth. Large continuous alpha grains result in early onset plastic deformation which mainly impact ductility. For columnar prior beta microstructures common in W-DED processing of Ti-6Al-4V, the directionality of the continuous alpha can result in severe anisotropy in ductility depending on how stress is applied. When the continuous alpha grains are subjected to a tensile opening stress mode, the deleterious effect on ductility is maximized [5]. This effect is observed when stresses are applied perpendicular to the build direction. Post-processing thermos-mechanical heat treatments are therefore typically required to minimize these effects on material properties.

This work explores two conventional post-process heat treatments for WAAM Ti-6Al-4V to investigate their impact on critical microstructure characteristics and the resulting anisotropy of the mechanical properties.

Experimental Methods

A billet of mill annealed Ti-6Al-4V was obtained from Bulk AM material which was processed and rolled in the x-direction. Ti-6Al-4V wire feed stock was purchased from United States Welding Corporation with the compositions of 6.75% Aluminum, 4.5% Vanadium, and 0.15% Iron. WAAM specimens were created using 1/8” tungsten electrode on a wirefeed AM printer, print parameters are shown in Table 01. Specimens for both WAAM and mill annealed were extracted using wire EDM, dimensions are shown in Figure 01.

Table 01: WAAM processing details.

Wire Feeder Parameters:	
Delay Time:	3.75 s
Feedrate:	200 mm/min Table Speed infill – 150 mm/min perimeter
Hatch:	5 mm
Layer Height:	1.25 mm
Wire Feed Speed:	1350 mm/min
6Al-4V ELI Ti Wire:	Wire and Rod 0.045” diameter Al = 6.75% Fe = 0.15 % V = 4.5% Ti Bal.

Specimens were extracted in three orientations related to the rolling and build direction as shown in Figure 01. Z-type specimens had their longitudinal axis perpendicular to the rolling direction in the xz-plane for the wrought material and parallel with the build direction in the xz-plane for the WAAM condition. For the wrought material, the X-type specimens had their longitudinal axis parallel to the rolling direction within the xy-plane with Y-type specimens were perpendicular to the rolling direction also within the xy-plane. For the WAAM condition both X-type and Y-type specimens were perpendicular to the build direction with there axis aligned with their respective directions within the xy-plane.

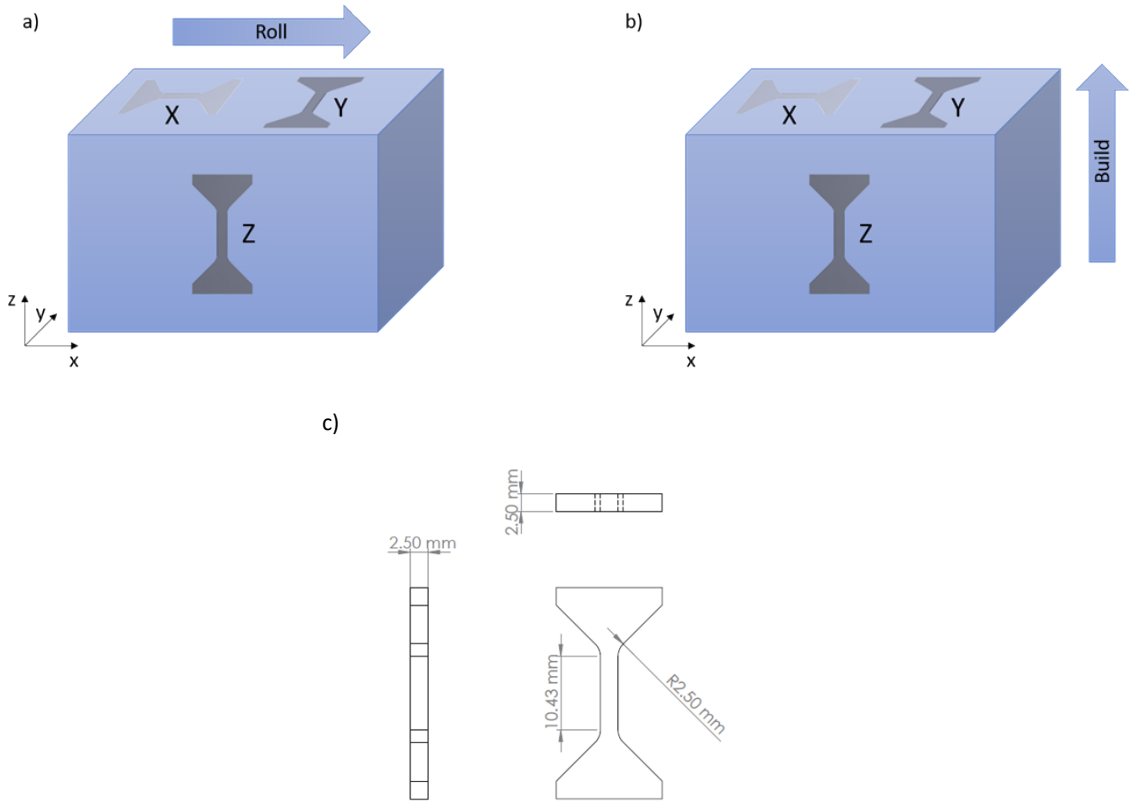

Figure 01: Direction of excised specimens from a) wrought Ti-6Al-4V, b) WAAM Ti-6Al-4V, and c) dimensions of wrought and WAAM Ti-6Al-4V high throughput tension specimens.

Specimens were nondestructively inspected using an immersion ultrasonic method using a Mistras Immersion tank with a 30 MHz 51 mm focal depth ultrasonic transducer probe. Immersion inspections were performed from the etched surface. The raster pattern used was done with a 50 µm resolution and at a height of 51 mm above the respective side being scanned.

This work explores two standard heat treatments specific for Ti-6Al-4V which are summarized in Table 02. Heat treatment 01 (HT-01) is a standard beta anneal with over-aging to better match the mill annealed condition. The second heat treatment (HT-02) is an alpha anneal also followed by an over-aging procedure. Before heat treatment the samples were lightly etched to remove the brass recast layer deposited to the specimens from the brass EDM wire. Following cleaning the samples were subjected to the respective heat treatments in a vacuum furnace and

quenched using Ar purge into the heating chamber. Both heat treatment schedules are shown in Figure 02.

Table 02: Heat Treatment schedules for both LB-DED processes.

HT ID	1-Max Temp. (°C)	1-Soak (min)	1-Quench	2-Max Temp. (°C)	2-Soak (min)	2-Quench
HT-01	1050	60	ArQ	725	120	ArC
HT-02	926	60	ArQ	725	120	ArC

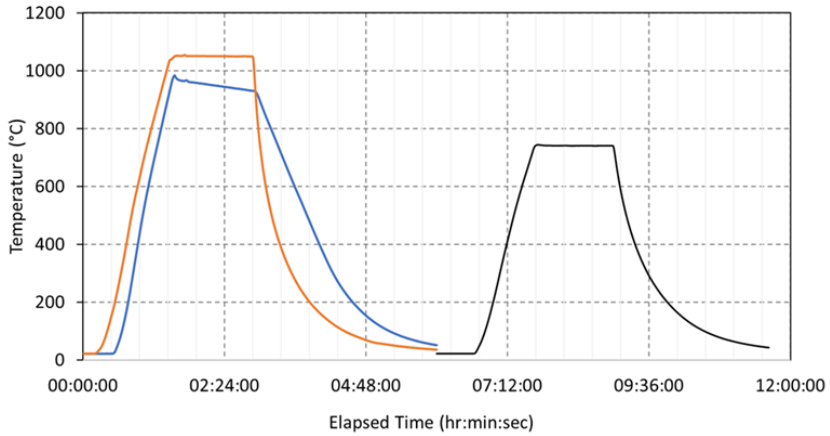

Figure 02: Heat treatment schedules for a) beta anneal (HT-01, orange) b) alpha anneal (HT-02, blue), and c) overage anneal (black).

Microstructural characterization was performed on a Zeiss Supra 55-VP FE-SEM equipped with Oxford Instruments X-Max SDD EDS and Symmetry EBSD detectors. EDS maps were collected at 20 kV across the entirety of the specimen build height, along the graded composition axis, to capture the full range of compositions, acquiring at least 10^6 counts per area. EBSD was performed at 20 kV for select regions to assess the grain and phase characteristics for all conditions.

Oxygen analysis was performed on a LECO ONH 836 Interstitial analyzer. All samples were placed in nickel capsules to aid in melting, then placed in a graphite crucible with graphite powder to convert any oxygen to carbon monoxide or carbon dioxide for analysis. Different quality control (QC) samples were measured to verify the analyzers were calibrated correctly. The QC's were run after the calibration, during the run, and after the run. All the QC's were well within the allowed range of the given value.

All samples were tested using the 1B Mini Bionix frame with a 5000lbf load cell. One camera (FLIR 90 fps, 4.1 MPix) was used to capture images of samples during testing. This camera captured images from the front of each tensile sample and had a 0.5x lens attachment with 12x zoom and a 1x adaptor.

Experimental Results

Mill Annealed Microstructures

The mill annealed condition grain morphology and phase distribution is shown in Figure 03 showing the YZ-plane perpendicular to the rolling direction. Figure 03(a) shows inverse pole figure (IPF) map illustrating the alignment of the grains in the -12-10 direction and partially recrystallized grains as indicated by the color gradient retained in many of the grains. Figure 03(b) shows the respective alpha + beta phases of the conventionally processed material. Approximately 5.9% of the beta phase is retained, as shown in blue. The average alpha grain size for the mill annealed condition is 5.32 µm.

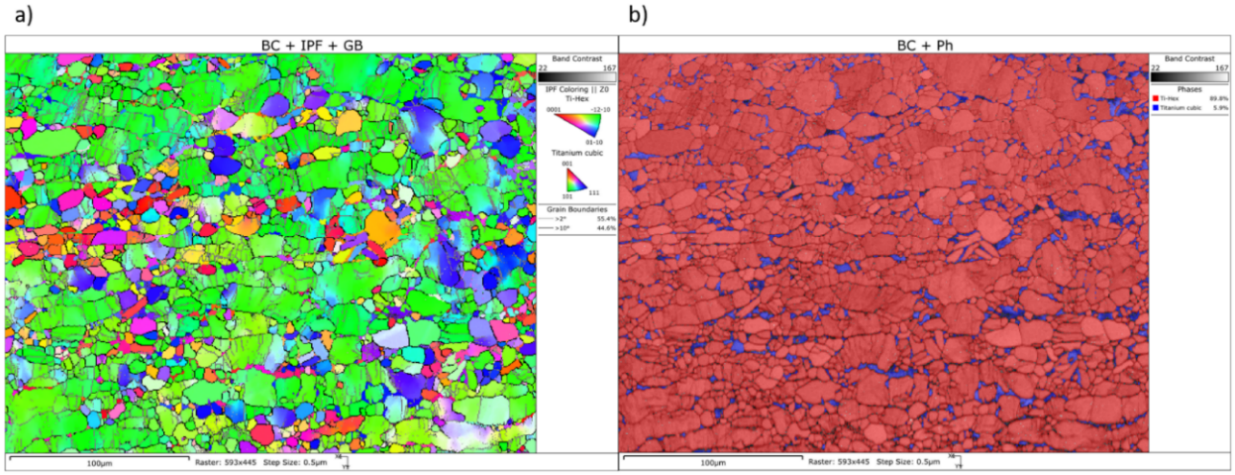

Figure 03: EBSD results of an excised wrought Ti-6Al-4V sample showing a) inverse pole figure and b) phase maps.

WAAM Microstructure

The WAAM process results in high solidification rates and martensitic β-to-α‘ transformation. This resulting microstructure can be observed in IPF map shown in Figure 04(a) as fine acicular grains. Compared to the mill annealed condition, Figure 04(b) reveals negligible retained beta for the as-built WAAM condition, <0.1%. The high cooling rates, which are directly correlated to the width of the acicular grains, result in an average grain width of 1.80 µm.

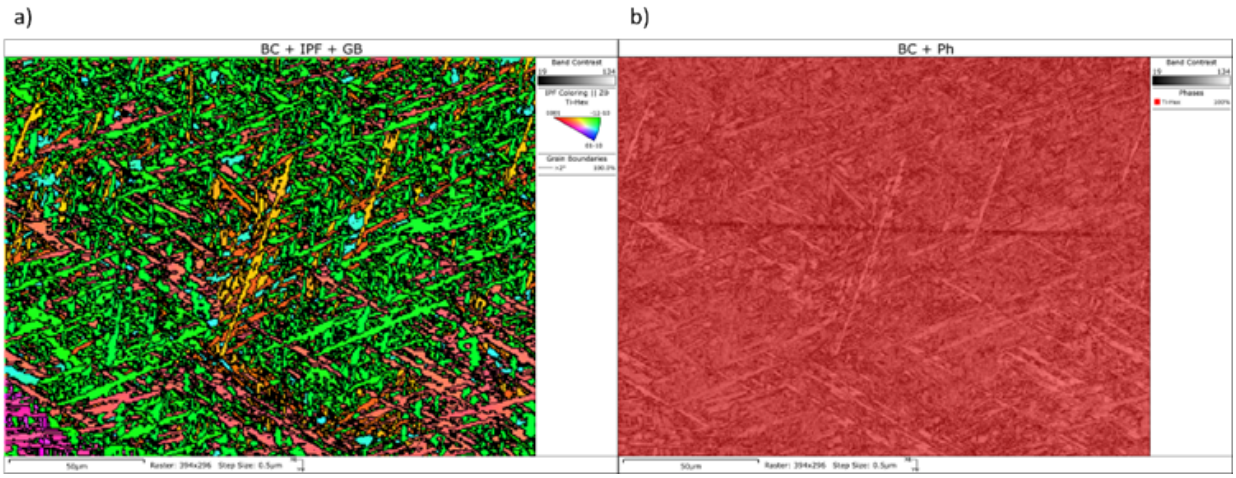

Figure 04: EBSD results of an excised WAAM sample showing a) inverse pole figure and b) phase maps.

The heat treatment effects on the resulting microstructure for the WAAM condition is shown in Figure 05. The alpha anneal stays below the beta transformation temperature (sub-transus) resulting in recrystallization of the martensitic α′ phase into a more typical alpha + beta microstructure for Ti-6Al-4V. The grains are a mixture of the lamellar and equiaxed grains as shown in Figure 05(a) with retained beta shown in Figure 05(b) as the blue regions mostly occurring at the grain boundaries of the alpha phase. Contrastingly, the beta anneal heat treatment surpasses the beta transformation temperature (super-transus) then is rapidly quenched resulting in the martensitic β-to-α‘ transformation shown in Figure 05(c), with similar morphology to the as-built condition. This again results in the fine acicular microstructure and negligible retained beta as shown in Figure 05(d).

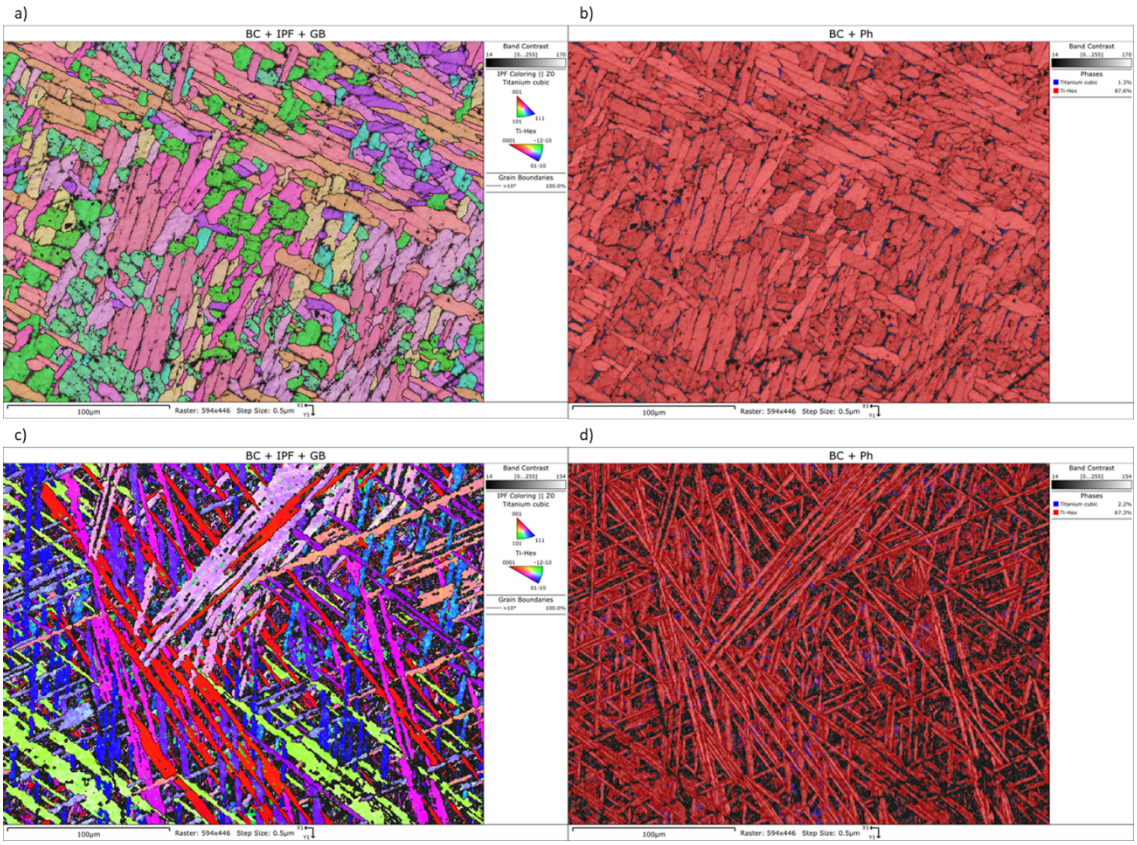

Figure 05: SEM results of a heat treated WAAM Ti-6Al-4V sample showing a) alpha annealed condition with associated b) phase distribution and c) beta-annealed condition with associated d) phase distribution.

Chemical Compositions

EDS was conducted on each material to document any major differences in chemical compositions since the wrought material and feedstocks originated from different sources. The results are tabulated in Table 03. The mill annealed condition Al composition was closer to 7 Wt.%, while the WAAM material was closer to 6 Wt.%. Oxygen analysis showed the wrought material had a higher oxygen concentration compared to the WAAM produced material, shown in Figure 06. Furthermore, oxygen results demonstrated that the heat treatments resulted in minimal increases in oxygen.

Table 03: Wrought and As-Built WAAM chemical compositions determined by EDS.

Wrought		**As-Built WAAM**	
Phase	**At. %**	**Phase**	**At. %**
Al	6.84	Al	6.05
V	3.77	V	3.68
Fe	0.14	Fe	0.12

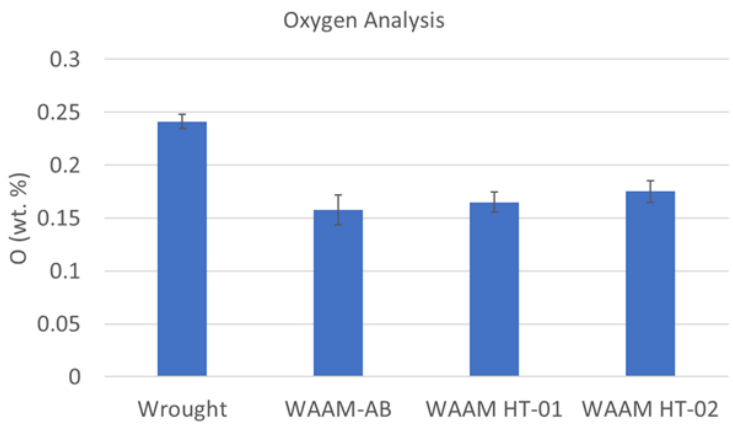

Figure 06: Oxygen Analysis for Wrought and WAAM As-Built, HT-01 and HT-02.

Porosity

For the mill annealed condition there were no significant pores found in any of the specimens. The ultrasonic inspection did identify significant pores in samples extracted in all orientations of the WAAM material. In some cases, the pores were in the shoulder or grip section while other pores were in the gage section of the specimens. Seven WAAM samples displayed significant pores.

Mechanical Properties

The stress-strain curves for the Wrought and as-built WAAM conditions are shown in Figure 07 along with box and whisker charts comparing the tensile properties for each condition. The total range of the respective property for the wrought material is outlined by the dotted lines. Briefly, the strengths of the wrought materials are noticeably lower than the wrought material while the ductility was lower on average but much closer to the range of the wrought material. In both cases some anisotropy was observed in yield stress and UTS. For the wrought condition the X-type specimen showed the highest average yield stress followed by Z-type and Y-type respectively. The box and whisker chart for yield stress suggests that the differences in each direction are significant as there is minimal overlap for each condition. The anisotropy in UTS for the wrought material was lower than yield stress with considerable overlap between the Y- and Z-type specimens. The X-type specimen, however, had the highest average strength which was determined to be significantly different from both Y- and Z-Type specimens. Interestingly the anisotropy in ductility did not appear to be significant though the averages for each type are noticeably different. There is considerable overlap between the box and whisker charts between all directions, suggesting these differences in averages are not significant. Conversely, the WAAM material showed lower strengths in Z-type specimens, both yield and UTS, but these were determined not to be significant as there is considerable overlap of the box and whisker data.

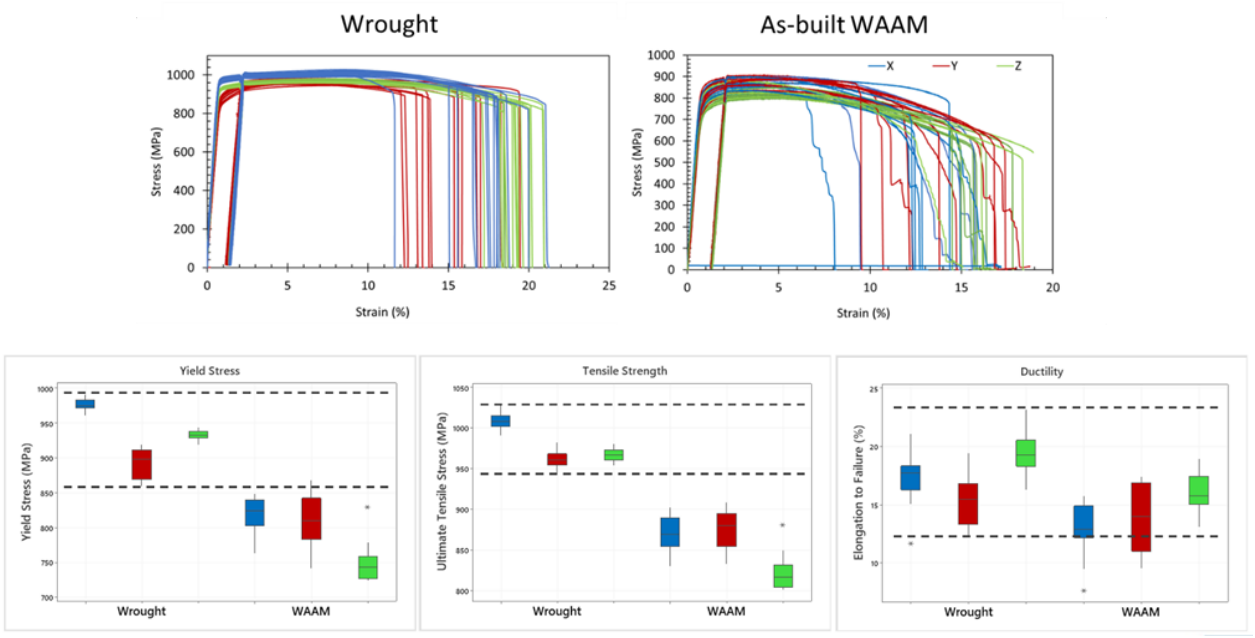

Figure 07: Tensile properties for Wrought and As-Built WAAM. Yield Stress, Ultimate Tensile Stress, and Elongation to Failure for Wrought and WAAM As-Built.

The stress-strain curves for the WAAM condition including all heat treatments are shown in the top images of Figure 08 with the respective box and whisker charts again provided below. All specimen directions are included in each graph. For the WAAM material both heat treatments resulted in significant decreases in ductility with the beta anneal (HT-01) resulting in a severe loss of ductility. The α anneal (HT-02) condition shows similar yield and UTS compared to the as-built condition while the beta annealed condition is so brittle that observations on the strength are difficult to determine.

The highest yield average stress and UTS occur in the Y-type specimens for both heat treatments and as-built conditions, however, the difference compared to the other directions is negligible. For yield stress the difference from the highest average stress to the lowest average stress is 8%. Similarly, the UTS only had a difference of 6% between the highest and lowest values. The elongation to failure showed the highest anisotropy between averages at 19%. The box and whisker charts suggests these differences in strengths were not significant while the ductility for X-type and Z-type specimens from HT-02 do appear to be significantly different. Again the beta annealed (HT-01) condition behaved in such a brittle manner that comparison of the mechanical properties for each direction are less reliable.

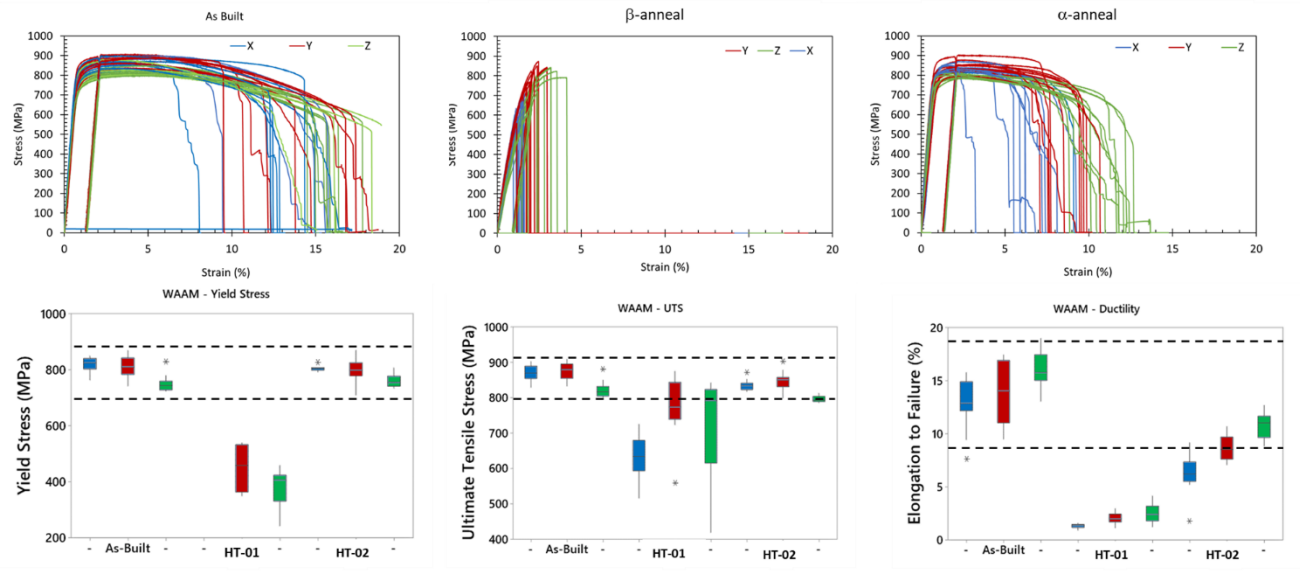

Figure 08: Tensile properties for all a) WAAM As-Built, b) WAAM alpha, and c) WAAM beta anneal. Yield Stress, Ultimate Tensile Stress, and Elongation to Failure for WAAM As-Built, WAAM alpha and WAAM beta anneal.

Discussion

One distinct observation comparing the mill annealed conditions to WAAM conditions are the higher strengths observed for the wrought material. This observation aligns with the observations made on the chemical analysis using EDS. The WAAM process resulted in approximately 12% lower concentration of aluminum which contributes to the solid solution hardening behavior of Ti-6Al-4V. While printing the WAAM samples the composition of aluminum decreased due to the high energy input and aluminum having a lower boiling temperature compared to the other elements in Ti-6Al-4V. In addition, the wrought Ti-6Al-4V material was found to have a much higher oxygen content as compared to the WAAM produced material. As an interstitial, oxygen is a known strengthening mechanism for Ti-alloys and therefore the higher strength for the wrought material is mostly attributed to the higher oxygen content.

The anisotropy for Ti-6Al-4V is often a major concern for additively manufactured materials which is typically sensitive to grain boundary alpha that preferentially forms at the prior-beta grain boundaries. Surprisingly, the lowest anisotropy was observed for the as-built WAAM material which suggests the cooling rate is sufficiently high to prevent large continuous alpha growth along these boundaries. The impact of the prior-beta microstructure and continuous alpha is still evident in the lower average ductility for the x and y-directions. Applying stress in these directions induces a tensile opening mode on the continuous alpha along the prior beta grains, resulting in early onset deformation and lower ductility. These differences in the as-built condition, however, are not considered to be significant.

Interestingly, the alpha anneal heat treatment did show significant anisotropy between the ductility in the X-type and Z-type directions, though there is considerable overlap with both directions compared to the Y-type data. This observation suggests that the sub-transus annealing

step did promote continuous alpha growth along the prior-beta grains. Figure 09 shows a representation of a continuous alpha grain for the alpha anneal condition. Continuous alpha results in a region where the slip length is much larger compared to the surrounding matrix. This size difference results in early onset plastic deformation when stresses are applied perpendicular to these continuous grains, resulting in the anisotropy observed.

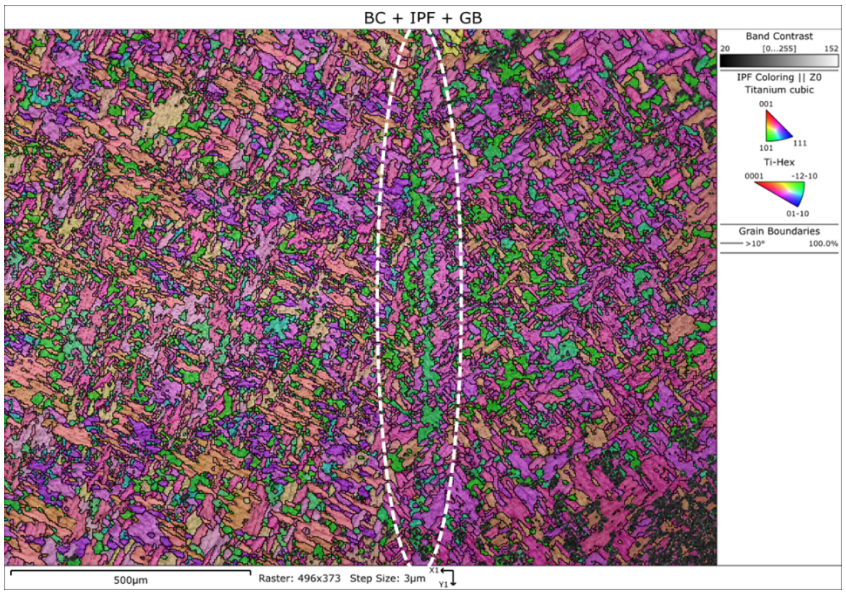

Figure 09: EBSD map of a continuous alpha grain along a prior beta grain resulting in increased anisotropy for the alpha anneal condition.

Surprisingly, the WAAM material demonstrates the best material properties in the as-built condition. Anisotropy increased for the alpha anneal (HT-02) because of continuous alpha growth along prior-beta grains. This observation was also accompanied by lower average elongation to failure in all directions. These observations demonstrate the important role the initial prior-beta microstructure plays in the mechanical properties of WAAM Ti-6Al-4V and how post-process heat treatments can magnify these effects. This also suggests that conventional heat treatment processes may not be appropriate for W-DED Ti-6Al-4V where columnar prior beta microstructures are present.

Conclusion

WAAM Ti-6Al-4V subjected to super-transus (HT-01) and sub-transus (HT-02) anneal and overaged heat treatments were compared to an as-built and conventionally processed material. Microstructural and mechanical properties in the three primary directions were analyzed and the following conclusions were made:

- WAAM material in the as-built condition showed more consistent mechanical properties across all directions compared to both post-process heat treatments.
- The as-built prior beta microstructure plays a dominant role in anisotropy with conventional post-processing heat treatments increasing these effects.

- Subsequent heat treatments for the WAAM material increased the oxygen content, however, the final content was still lower than the mill annealed material, resulting in lower strength.
- Nondestructive inspection for the WAAM condition suggests porosity does not significantly impact the mechanical performance.

Results from this study demonstrate that the performance of the WAAM Ti-6Al-4V in the as-built condition is mostly consistent. One note is that the high throughput testing utilized in this study provides a rapid means of comparison between various material conditions, however, the analysis is restricted to comparison of the miniature test specimens. To establish true design properties additional efforts are required that strictly follow established testing, and qualification standards.

References

[1] B. Baufeld, E. Brandl and O. Van der Biest, "Wire based additive layer manufacturing: Comparison of microstructure and mechanical properties of Ti–6Al–4V components fabricated by laser-beam deposition and shaped metal deposition," *Journal of Materials Processing Technology,* pp. 1146-1158, 2011.

[2] F. Martina, J. Mehnen, S. Williams and P. Colegrove, "Investigation of the benefits of plasma deposition for the additive layer manufacture of Ti–6Al–4V," *Journal of Materials Processing Technology,* pp. 1377-1386, 2012.

[3] F. Wang, S. Williams and M. Rush, "Morphology investigation on direct current pulsed gas tungsten arc welded additive layer manufactured Ti6Al4V alloy.," *The International Journal of Advanced Manufacturing Technology,,* pp. 597-603, 2011.

[4] D. Yuan, S. Shao, C. Guo, F. Jiang and J. Wang, "Grain refining of Ti-6Al-4V alloy fabricated by laser and wire additive manufacturing assisted with ultrasonic vibration," *Ultrason Sonochem,,* 2021.

[5] B. E. Carroll, T. A. Palmer and A. Beese, "Anisotropic tensile behavior of Ti–6Al–4V components fabricated with directed energy deposition additive manufacturing.," *Acta Materialia,* pp. 309-320, 2015.